INTERNATIONAL ATOMIC ENERGY AGENCY
UNITED NATIONS EDUCATIONAL, SCIENTIFIC AND CULTURAL ORGANIZATION

INTERNATIONAL CENTRE FOR THEORETICAL PHYSICS
34100 TRIESTE (ITALY) - P.O.B. 586 - MIRAMARE - STRADA COSTIERA 11 - TELEPHONES: 224281/2/3/4/5/6
CABLE: CENTRATOM - TELEX 460392-I

SMR/110/A - 4

WORKING PARTY

ON

"PHYSICS OF CONDENSED MATTER AT PLANETARY PRESSURES"

(20 August - 7 September 1984)

POLYMORPHIC TRANSITIONS

III : Mineralogy and petrology of the Earth's mantel

A.B. THOMPSON

Dept. für Erdwissenschaften
E.T.H. Zürich, CH-8092
Switzerland

Ringwood (1975)

Table 11-7 RELATIVE VOLUMES OF A_2BO_4 POLYMORPHS. (*From Reid and Ringwood, 1970*)

Structure type	Examples, with coordination numbers,* of metals and anions	V/V_o†	$\Delta V/V_o$(%)‡
Olivine [α]	$^{[6]}Mg_2{}^{[4]}Si^{[4]}O_4$	1.20	20
β-Mg_2SiO_4 type	$^{[6]}Co_4{}^{[4]}Si_2{}^{[4]}O_6{}^{[5]}O_1{}^{[3]}O_1$	1.11_5	11.5
Spinel A_2BO_4[γ]	$^{[6]}Fe_2{}^{[4]}Si^{[4]}O_4$	1.09	9
Spinel AB_2O_4	$^{[4]}Mg^{[6]}Al_2{}^{[4]}O_4$	1.07_5	7.5
$2AO + BO_2$	$2^{[6]}Mg^{[6]}O + {}^{[6]}Ti^{[3]}O_2$	1.00	0
$AO + B_2O_3$	$^{[6]}Mg^{[6]}O + {}^{[6]}Al_2{}^{[4]}O_3$	1.00	0
Sr_2PbO_4 [δ]	$^{[6]}Mn_2{}^{[6]}Ge^{[5]}O_2{}^{[4]}O_2$	1.00	0
$CaMn_3O_4$	$^{[8]}Ca^{[6]}Mn_3{}^{[5]}O_2{}^{[6]}O_1{}^{[4]}O_1$	0.98	− 2
Defect NiAs§	$^{[6]}Fe^{[6]}Cr_2{}^{[5]}S_2{}^{[4]}S_2$	0.98	− 2
K_2NiF_4	$^{[8]}Ca_2{}^{[6]}Ge^{[6]}O_4$	0.96_5	− 3.5
$CaFe_2O_4$	$^{[8]}Ca^{[6]}Al_2{}^{[5]}O_4$	0.94_4	− 5.5
$CaTi_2O_4$	$^{[8]}Ca^{[6]}Ti_2{}^{[5]}O_2{}^{[6]}O_1{}^{[4]}O_1$	0.94_5	− 5.5
Ca_2IrO_4	$^{[9]}Ca_2{}^{[7]}Ca_3{}^{[6]}Ca_1{}^{[6]}Ir_3{}^{[6]}O_3{}^{[5]}O_8$	0.93_5	− 6.5

*Coordination number given by superscripts in brackets.
†Structure volumes relative to sum of constituent oxide volumes, averaged from Fig. 11-14.
‡$\Delta V = V - V_o$.
§A_2BO_4 type not as yet obtained for oxides.

Table 16.1

Table 1. High-pressure ^{IV}Si → ^{VI}Si transformations.

Formula	^{IV}Si phase	^{VI}Si phases	Transition pressure, P_T (kbar)	Density increase* (%)	$\bar{\beta}_{Si-O}$† (Mbar^{-1})	d_o(Si–O) (Å)	d_{P_T}(Si–O)‡ (Å)	Reference
SiO_2	Coesite	Stishovite	80 ± 2	50	0.13	1.610	1.59	(7)
Al_2SiO_5	Kyanite	Corundum + stishovite	160 ± 20	11	0.13	1.630	1.595	(9)
$MgSiO_3$	Clinoenstatite → [stishovite + β-Mg_2SiO_4] →	Ilmenite-type	[170] → 250	[10] → 10	[0.13] → 0.15	[1.630] → 1.655	[1.59] → 1.59	(10, 11)
$FeSiO_3$	Clinoferrosilite → [stishovite + γ-Fe_2SiO_4] →	Wustite + stishovite	[150] → 250	[10] → 10	[0.13] → 0.15	[1.630] → 1.655	[1.59] → 1.59	(12)
$CaSiO_3$	Wollastonite	Perovskite-type	160		0.13	1.630	1.595	(13)
$ZnSiO_3$	Zinc pyroxene	Ilmenite-type	180		0.13	1.630	1.59	(11)
Mg_2SiO_4	Magnesium silicate spinel	Perovskite-type + periclase	270	~10	0.15	1.655	1.59	(10)
Fe_2SiO_4	Ferrous silicate spinel	Wüstite + stishovite	~250	~10	0.15	1.655	1.59	(12)
Ni_2SiO_4	Nickel silicate spinel	NiO + stishovite	190		0.15	1.655	1.61	(14)
Co_2SiO_4	Cobalt silicate spinel	CoO + stishovite	180 ± 10		0.15	1.655	1.61	(15)
$NaAlSi_2O_6$	Jadeite	$NaAlSiO_4$ (calcium ferrite-type)+ stishovite	180	19	0.13	1.625	1.59	(16)
$KAlSi_3O_8$	Orthoclase → [kyanite + coesite + $K_2Si_4O_9$ (wadeite-type)] →	Hollandite-type	[~60] → 100	[25] → 25	[0.13] → 0.13	[1.610] → 1.610	[1.595] → 1.59	(17)
$Mg_3Al_2Si_3O_{12}$	Pyrope	Ilmenite-type	245 ± 5	7	0.11	1.635	1.59	(18)

*Density increases at 1 atm, 23°C. †$\bar{\beta}_{Si-O} = [d_o(Si–O) - d_{P_T}(Si–O)]/[d_o(Si–O) \times P$ (Mbar)]. This is the mean linear Si–O compressibility as determined from high-pressure x-ray studies; d_{P_T}(Si–O) is the Si–O distance under transition conditions and d_o(Si–O) is the distance under room conditions. ‡The Si–O distance at P_T is predicted by $d_{P_T}(Si–O) = d_o(Si–O)[1 - \bar{\beta}_{Si-O} \times P_T]$. §Bracketed quantities refer to transformation from ^{IV}Si to mixed ^{IV}Si + ^{VI}Si assemblages. Calculations for both ^{IV}Si → ^{IV} + ^{VI}Si and ^{IV} + ^{VI}Si → ^{VI}Si are presented.

0036-8075/78/0922-1122$00.50/0

Table 16.2

Hazen + Finger (1978)

Tables 16.1 16.2

MANTLE PHASES

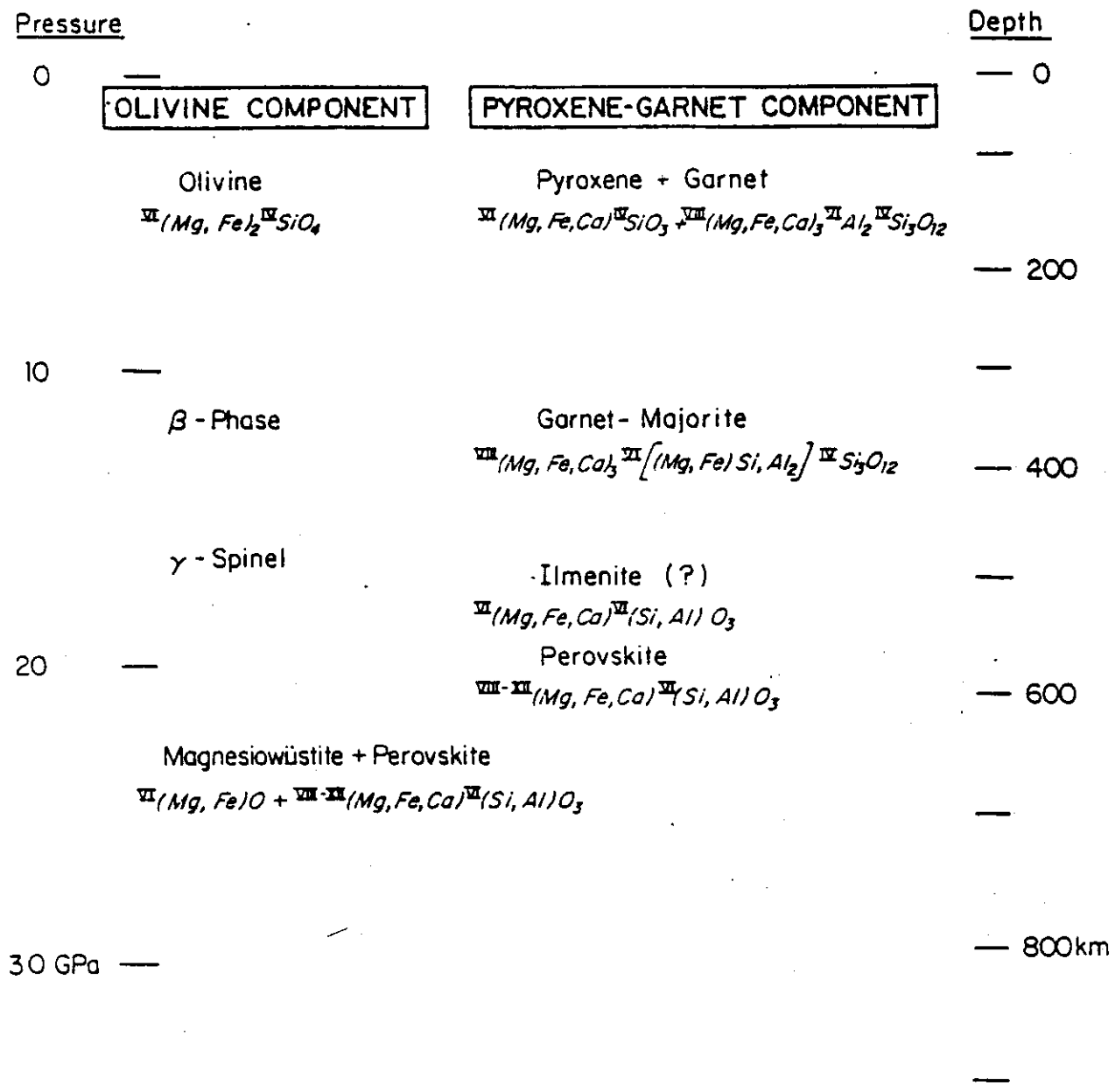

Fig 16.1

Fig. 1. Summary of mineral phases corresponding to the olivine component and the pyroxene-garnet component of an upper-mantle assemblage as a function of pressure (or equivalent depth in the mantle), based on the work summarized by *Akimoto et al.* [1976], *Liu* [1979*a*], and *Yagi et al.* [1979]. Crystal-chemical formulae indicating the coordination numbers of the cations (Roman numeral superscripts) are included under the corresponding names of the structure types to illustrate the increase in coordination with depth (the formulae of β-phase and γ-spinel are identical to the formula of olivine). The question mark indicates that the ilmenite structure may not be stable for aluminous mantle compositions at high pressures (see text).

Jeanloz and Thompson, 1983

16·1

Dziewonski Anderson (1981) Phys Earth Planet Int 25, 297-356

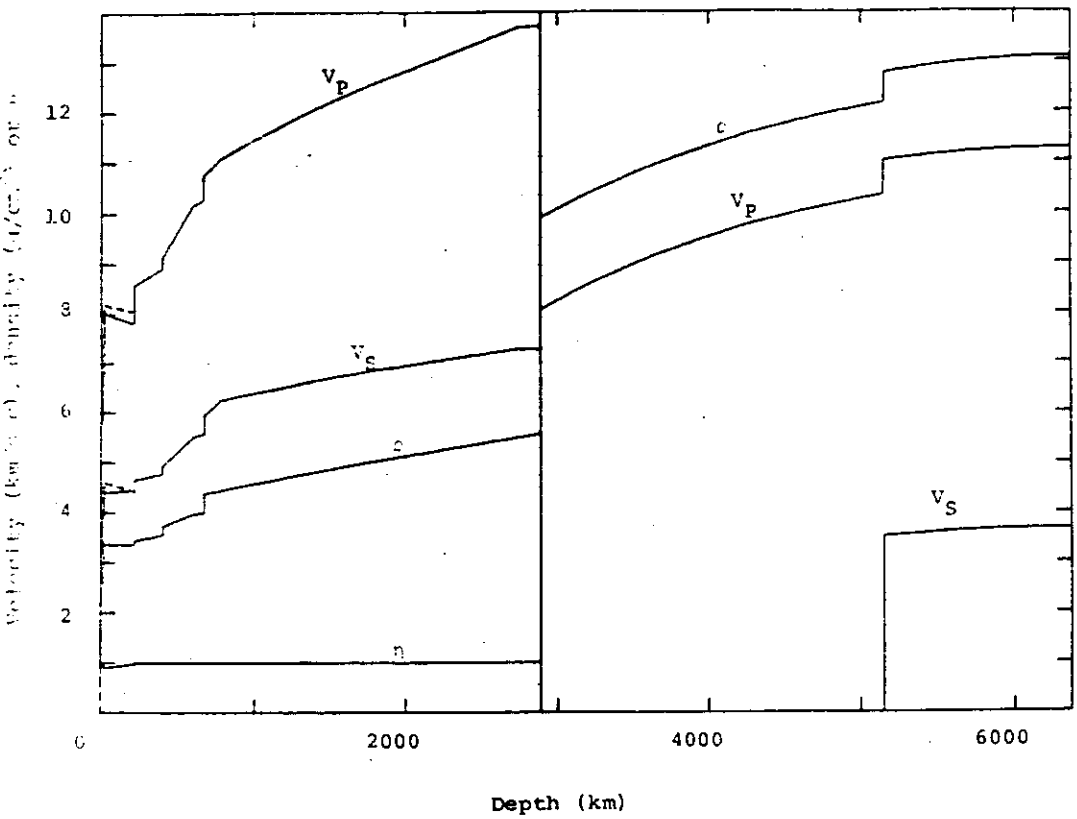

8. The PREM model. Dashed lines are the horizontal components of velocity. Where η is 1 the model is isotropic. The core is opic.

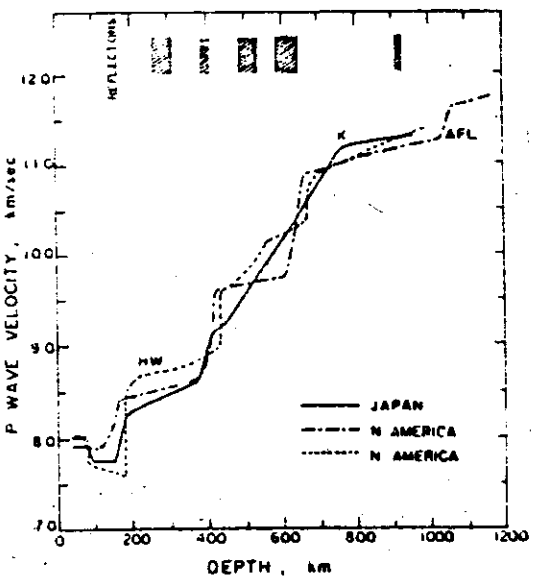

Figure 18. Distribution of seismic P wave velocities in the outer 1200 km of the mantle. Curves designated by K, AFL and HW represent the models proposed by Kanamori (1967) for the Japanese Islands, by Archambeau, Flinn and Lambert (1969) for the Western continental United States, and by Helmberger and Wiggins (1971) for the midwestern United States, respectively. Reflecting zones proposed by Whitcomb and Anderson (1970) are also indicated in the upper part of the figure

Akimoto et al (1976)
Phys chem min Rocks ed. Strens

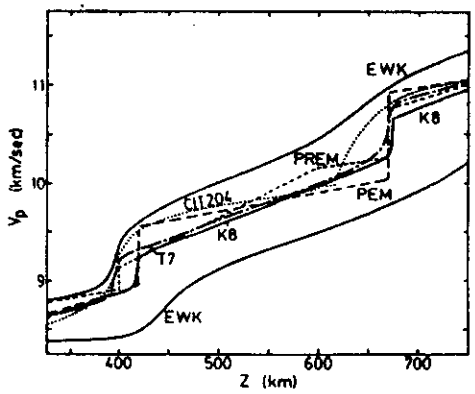

Fig. 7. Seismically observed compressional velocity profiles of the mantle transition region from various authors: EWK, velocity bounds of *England et al.* [1977]; CIT204, *Johnson* [1967]; PREM, *Dziewonski and Anderson* [1981]; PEM, *Dziewonski et al.* [1975]; K8, *Given and Helmberger* [1980]; T7, *Burdick and Helmberger* [1978].

Lees et al (1983)
J. Geophys. Res. 88
8145-8159

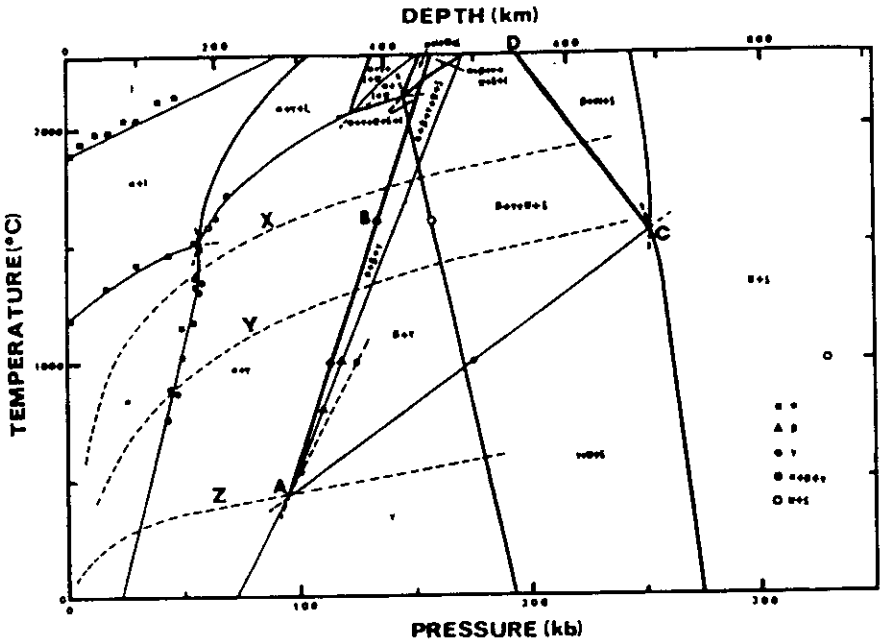

Fig. 5. Proposed phase diagram for the pseudo-binary system Mg_2SiO_4—Fe_2SiO_4. Plotted data and symbols for the phases are shown in Table I. Fine and coarse lines are univariant lines for one component system (Mg_2SiO_4 or Fe_2SiO_4), and for two (Mg_2SiO_4—Fe_2SiO_4, MgO—SiO_2, or FeO—SiO_2) or three (MgO—FeO—SiO_2) component systems, respectively. $AB(\alpha + \beta + \gamma)$ and $CD(\beta + \gamma + w + s)$ are univariant lines responsible for 400-km and 650-km discontinuities, respectively. X and Y are the range of geotherms under continental and oceanic plates (Ahrens, 1972). Z is the geotherm of the coldest part of a fast plunging [illegible] (Minotte and Schubert, 1973).

Sung and Burns (1976)

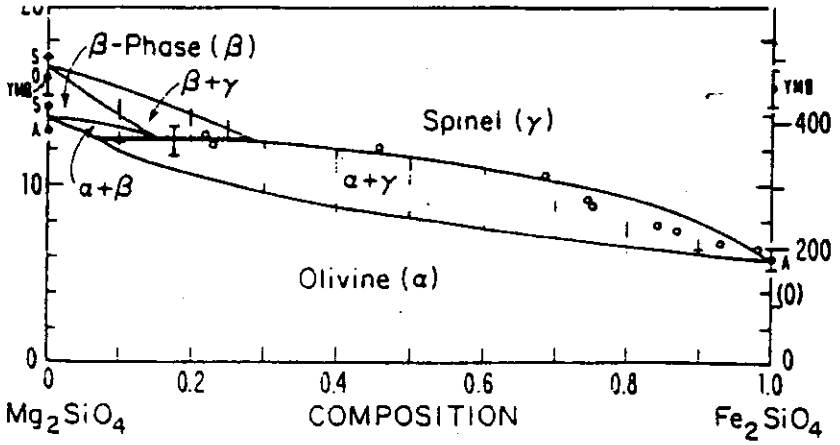

16.4

Fig. 6. Isothermal (P-X) phase relations along the olivine join in the system MgO-FeO-SiO_2 at approximately 1000°C. The composition of the upper mantle and the depth in the earth corresponding to the pressure scale (right-hand) scale are also shown. Abbreviations for each phase are given in parentheses next to the mineral name labeling the appropriate field of stability. The dashed curves represent tentative extrapolations of the phase equilibria to high pressures (see text). The data of *Akimoto and Fujisawa* [1968] and *Kawada* [1977] for the α-β-γ equilibria are summarized as short vertical lines (pressures for a phase boundary, at a given composition, consistent with the quench experiments; dotted where uncertain) and open circles (compositions of γ-spinel coexisting with olivine at the indicated pressure based on X ray lattice parameters of the quenched samples). Discontinuous reactions are shown as heavy horizontal lines at constant pressure. The data of *Akimoto* [1972] (A), *Ohtani* [1979] (O), *Suito* [1977] (S), *Yagi et al.* [1978, 1979] (YMB), and *Jeanloz and Ahrens* [1980] (JA) are indicated as solid circles. Estimated uncertainties are shown by the error bars.

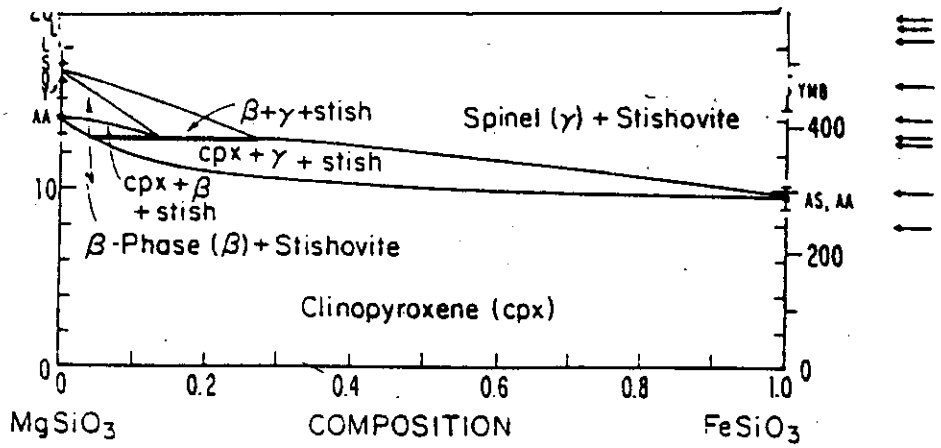

16.6

Fig. 7. Isothermal (P-X) phase relations along the pyroxene join of the system MgO-FeO-SiO_2 at approximately 1000°C. The format is as in Figure 6, and the phase boundaries in these two figures are consistent with the data of *Nishizawa and Akimoto* [1973]. The data of *Akimoto and Syono* [1970] (AS), *Akaogi and Akimoto* [1977, 1979] (AA), *Yagi et al.* [1978, 1979] (YMB), and *Liu* [1976*b*, 1977*a*, 1979*a*] (L) are included. The lowest pressure at which silicate perovskite appears is uncertain (open circle).

Jeanloz + Thompson 83

16.4 | 16.6

MgO - FeO - SiO_2 Ternary Diagram Figure

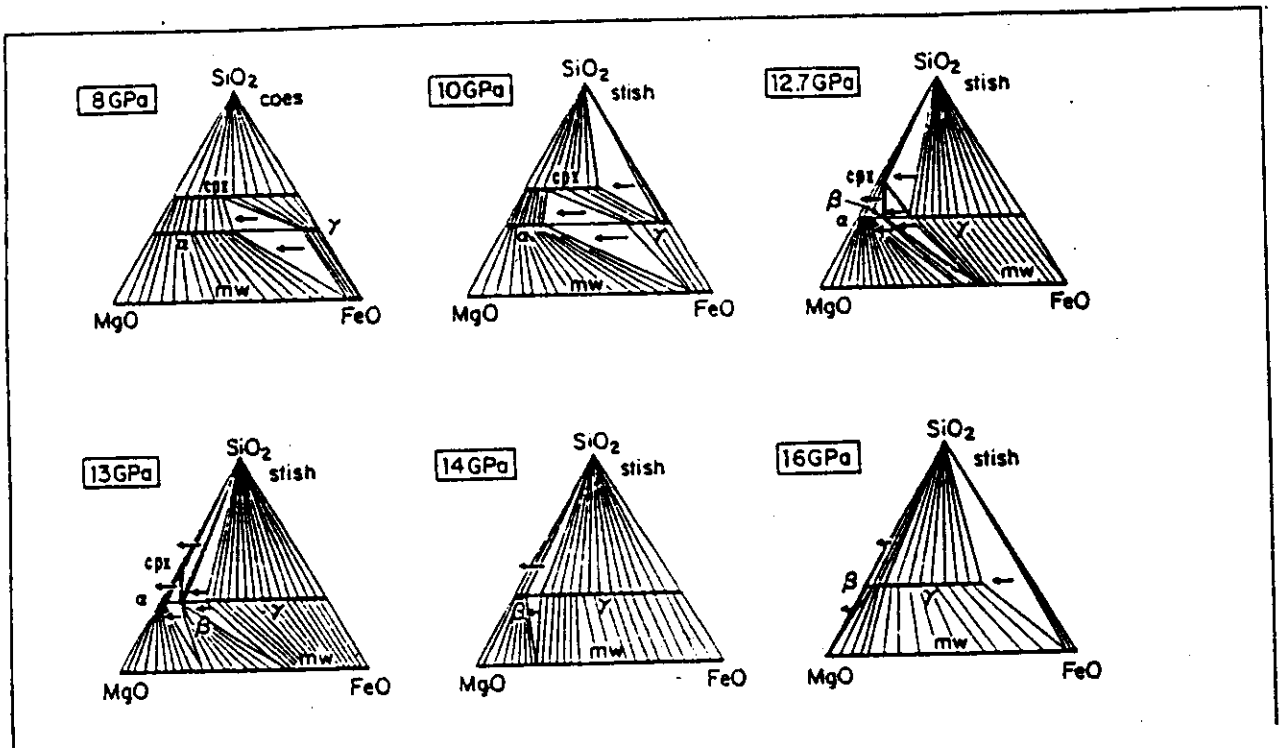

16.5

Fig. 8. Isothermal sections at approximately 1000°C of the MgO-FeO-SiO_2 system at the pressures indicated by arrows on the right-hand sides of Figures 6 and 7. The range of plausible compositions for the upper mantle is given in the key, and the effect of increasing pressure on the displacement of compositions of the three-phase regions is shown by the horizontal arrows.

Fearley + Thompson

16.11

16.11 | 16.5

Jaques & Thompson 83

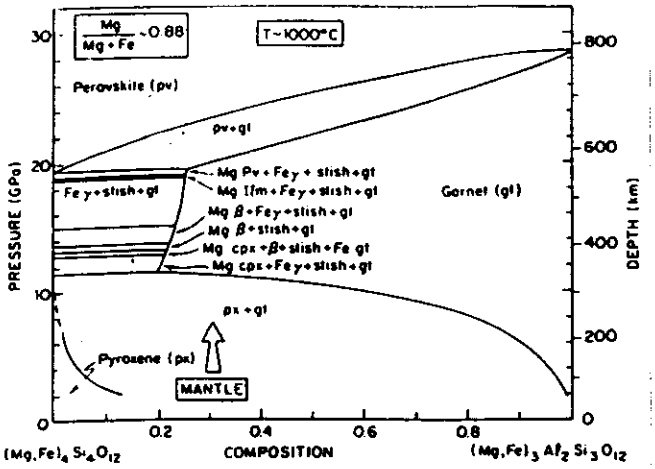

16.7

Fig. 13. Tentative pseudobinary, isothermal phase diagram between pyroxene and garnet components in the system MgO-FeO-SiO_2-Al_2O_3 at approximately 1000°C. The ratio $x_{Mg} = Mg/(Mg + Fe) = 0.88$ is appropriate for the upper mantle. Complexities of the low-pressure equilibria have been ignored [cf. *Boyd and England*, 1964; *Kushiro et al.*, 1967; *Arima et al.*, 1974; *Banno*, 1974; *Raheim and Green*, 1974; *Thompson*, 1979]. The data of *Liu* [1975c, 1977a] and *Akogi and Akimoto* [1977, 1979] have been used or extrapolated on the basis of the equilibria summarized in Figures 6 and 7.

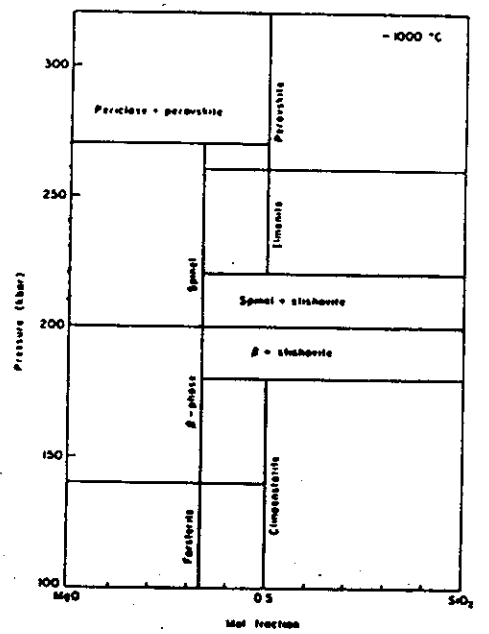

Fig. 3. Schematic isothermal phase diagram for the system MgO-SiO_2. (After Liu, 1976a.)

Fig. 3. A proposed pressure-composition phase diagram for the MgO-SiO_2 system: *Ol*, olivine; *β*, *β*-phase; *Sp*, spinel; *Cpx*, clinoenstatite; *Opx*, orthoenstatite; *Cs*, [illegible] low quartz;

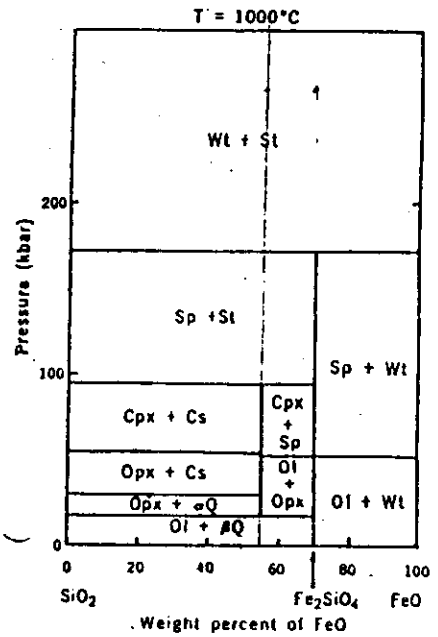

Fig. 2. A proposed pressure-composition phase diagram for the FeO-SiO_2 system: *Ol*, olivine; *Sp*, spinel; *Cpx*, clinoferro-

Replace this with
Liu 76 - ilm/psk.

Murg + Bassett 75

16.8a

16.8b

16.7
16.8a 16.8b

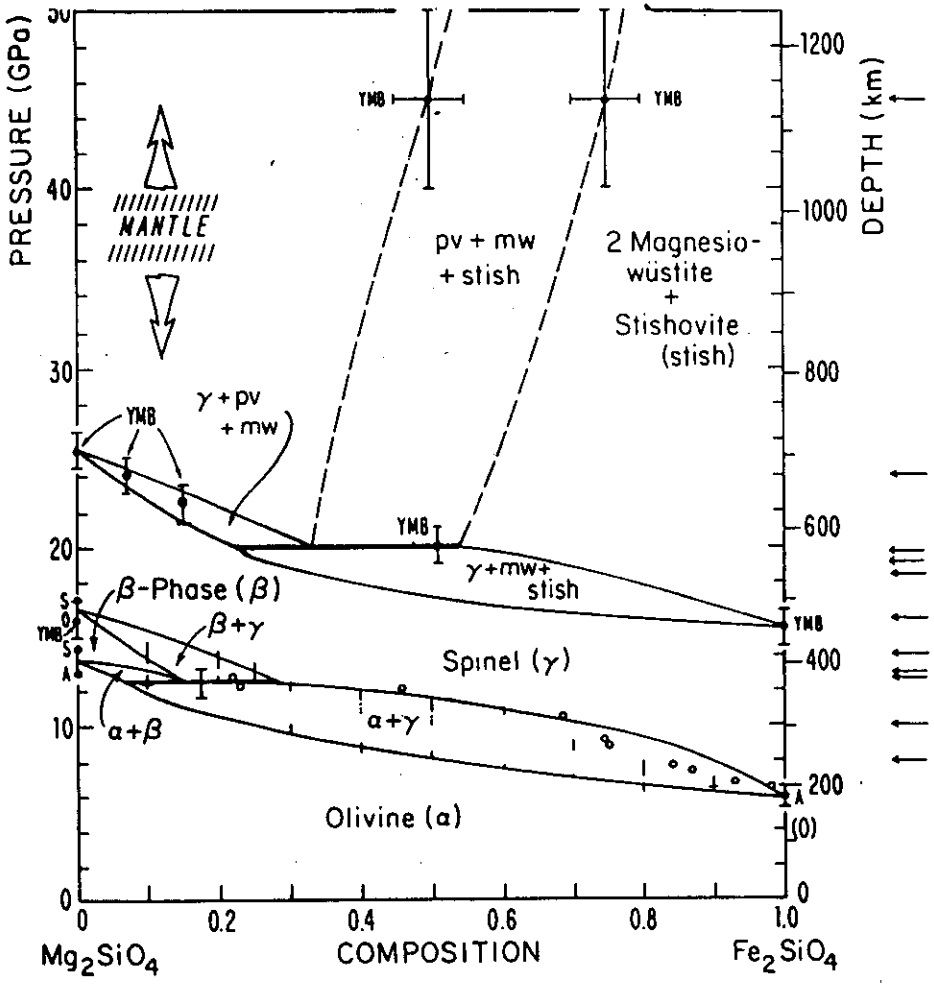

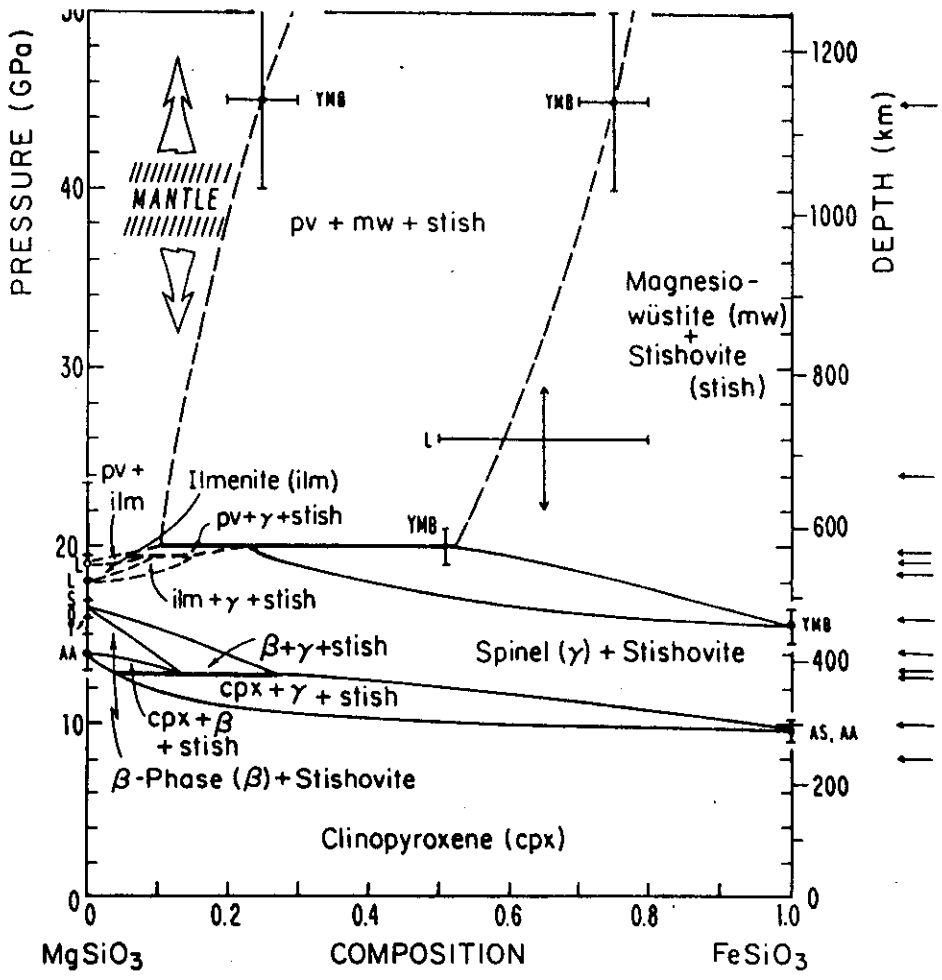

Jeanloz + Thompson 87

16.9

16.10

16.9

16.10

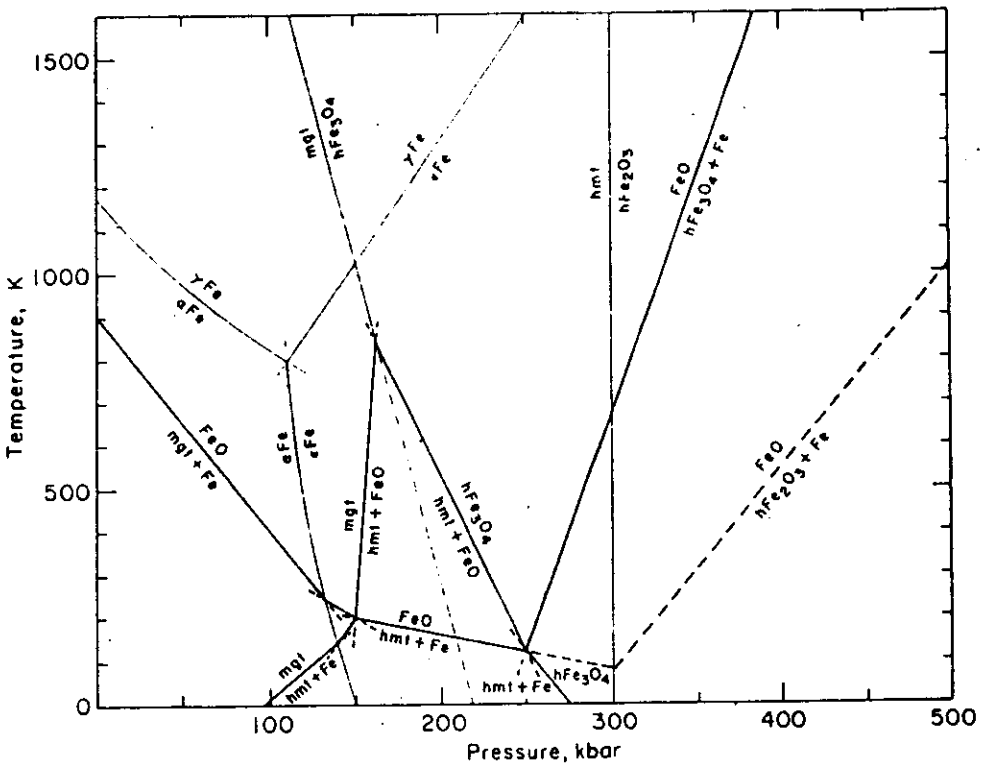

Fig. 4. Estimated phase diagram of Fe–O. *Heavy curves:* binary univariant; *Light curves:* degenerated unary univariant; *Dotted curves:* metastable extensions. The α–γ–ϵFe boundaries are from Bundy (1965). The magnetite (mgt) to high-pressure Fe_3O_4 (hFe_3O_4) boundary is estimated at between 25 and 300°C from the data of Mao et al. (1974). Sluggishness of the reaction is considered. The hematite (hmt) to high-pressure Fe_2O_3 (hFe_2O_3) boundary is arbitrarily set as a vertical line at 300 kbar, because shock-wave data indicate only that the reaction is below 600 kbar and no temperature coefficient is available. The hmt–h Fe_2O_3 transition was not observed in the diamond cell below 300 kbar

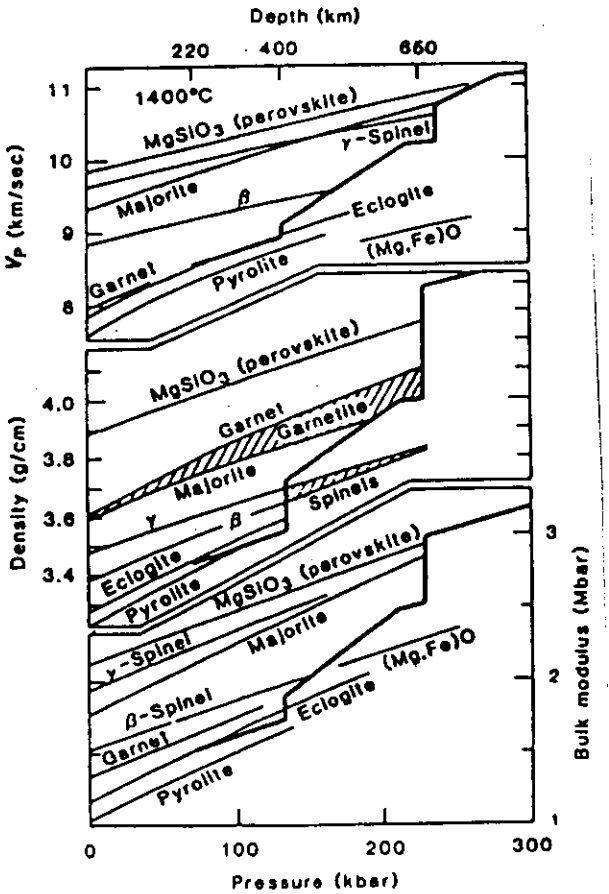

Fig. 2. Compressional velocity (V_P), density, and bulk modulus (K) of upper mantle (heavy line) for the earth model PREM compared with values calculated for various minerals and mineral assemblages along a 1400°C adiabat. Olivine is in the β-spinel structure near 400 km, in the γ-spinel structure at 650 km, and in the perovskite plus (Mg,Fe)O structure below 650 km. An olivine-rich mantle can therefore be ruled out over this depth range. An eclogite mantle should lie between garnet or eclogite and majorite (Al_2O_3-poor garnet) between 400 and 670 km, and this is permitted by the data. The lower mantle is best fit by perovskite, with only minor (Mg,Fe)O.

Anderson (1984)

9

Mao + Bell 1977
Energetics of Geological Process
Saxena eds
Bhattacharji
Springer

16.12

16.12

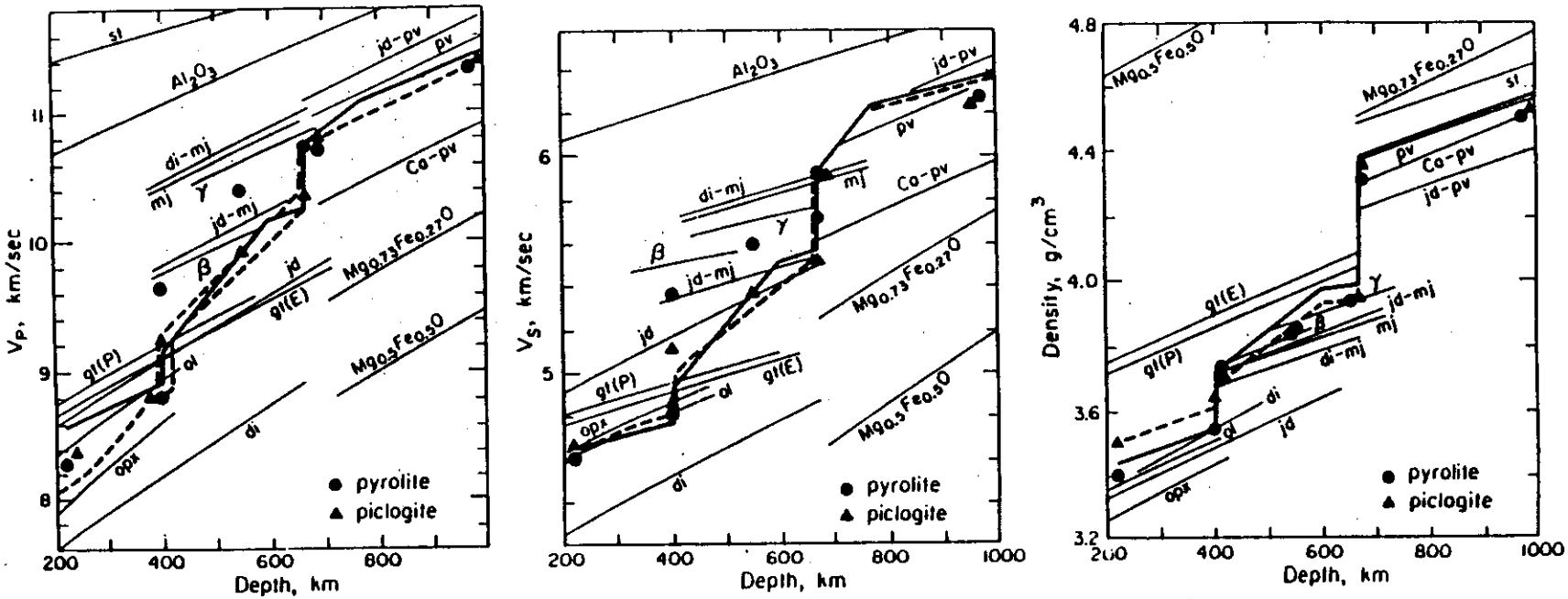

Compressional velocity (V_p), shear velocity (V_s) and density as a function of depth, for various candidate mantle phases. The average Earth model PREM is shown (heavy solid line) along with a range of velocities observed from several regional body wave studies (dashed lines, references in text). The dashed density profile is a perturbation of PREM which satisfies the mean Earth density and, with negligible error, moment of inertia. The mean upper mantle + transition zone density is the same as PREM. Adiabats are initiated at T = 1400°C (at P = 0). All Mg-Fe bearing phases contain 10% Fe^{2+} with the exception of garnet, majorite and $Mg_xFe_{1-x}O$. Circles and triangles indicate the properties of pyrolite and picritic eclogite, or piclogite (cpx + gt >> ol + opx), mineral assemblages, respectively. Note that the seismic velocity profiles are substantially lower than pyrolite velocities (predominately beta, or gamma, + mj) between 400-670 km, but are well matched by piclogite. Velocity jumps for pyrolite do not satisfy the 400 and 670 km discontinuities. $Mg_{0.73}Fe_{0.27}O$ and $Mg_{0.5}Fe_{0.5}O$ are appropriate for perovskite-bearing piclogite and pyrolite compositions, respectively. Abbreviations: ol, olivine; opx, orthopyroxene; di, diopside; jd, jadeite; gt (E,P), garnet (eclogite, pyrolite); mj, opx composition majorite; di-or jd-mj, diopside or jadeite composition majorite; pv, $Mg_{0.9}Fe_{0.1}SiO_3$-perovskite; jd- or Ca-pv, jadeite or $CaSiO_3$ composition perovskite; st, stishovite.

Bass & Anderson (1984)

V-13

10

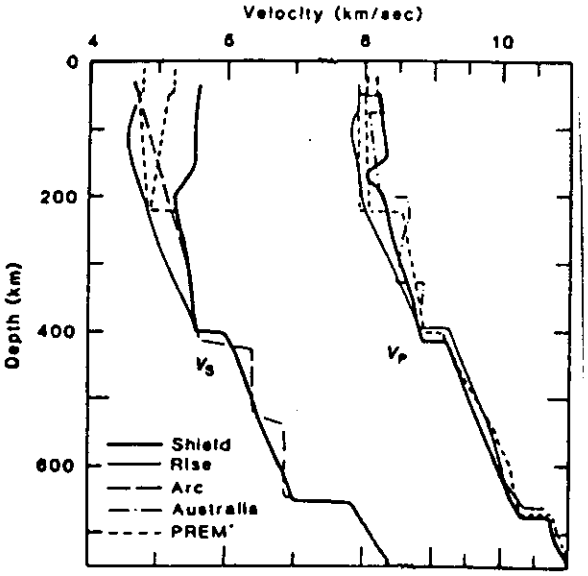

Fig. 1. Compressional (V_P) and shear (V_S) velocities as a function of depth for various tectonic provinces (*35–38*). The shield structures have velocities that are faster than those in other regions to depths of 150 to 220 km. The complications in this depth range probably result from a change in chemistry and the associated thermal boundary layer. The rise model is for the northern part of the East Pacific Rise and is slow to a depth of 400 km, suggesting a deep origin for midocean-ridge basalts. The PREM' model is a modification of the average earth model PREM, which is anisotropic above 220 km; the two short dash curves for PREM' represent horizontal and vertical propagation. The high gradients between 400 and 650 km may be due to the diopside-majorite transition.

16.14

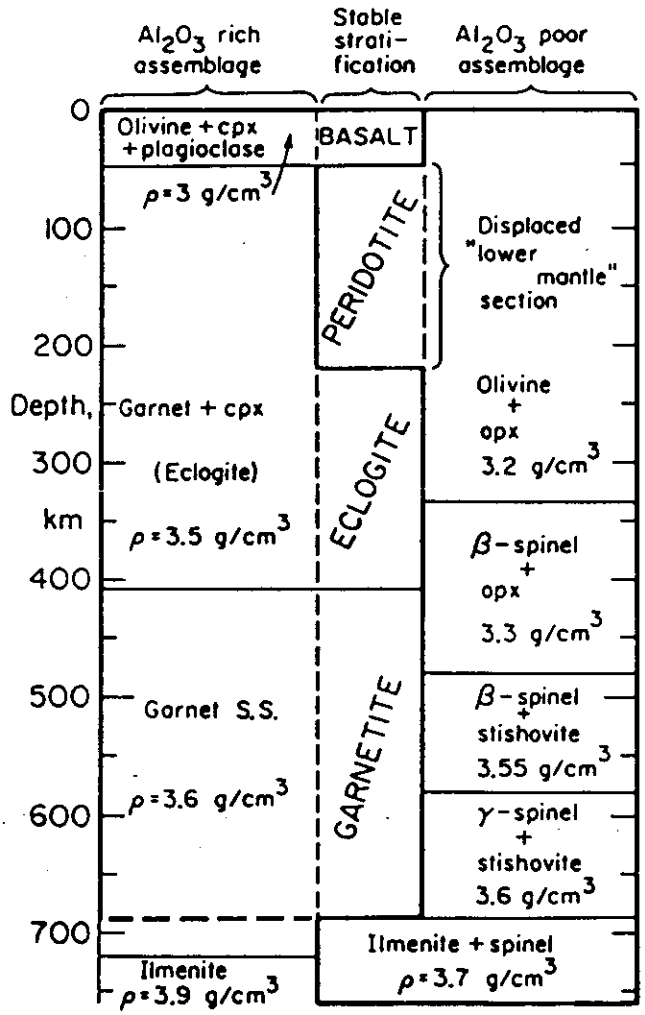

Figure 1. Zero pressure densities of basalt-eclogite (left) and peridotite (right) taken as a 1:1 mix of $MgSiO_3 \cdot Mg_2SiO_4$. The center column gives the gravitationally stable configuration. The broad stability field of garnet prevents eclogite from sinking below about 670 km.

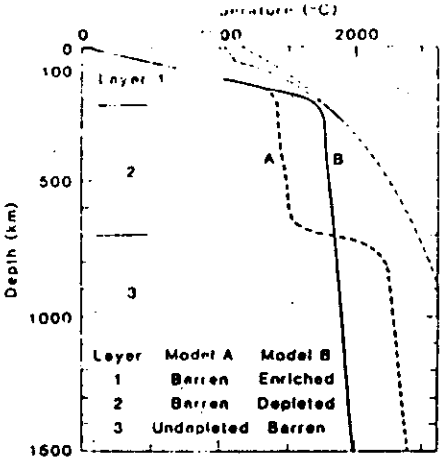

Fig. 4. Schematic diagram of mantle geotherms for two types of layered models. Model A has a very depleted, or barren, upper mantle and a primitive or undepleted lower mantle (high uranium, thorium, and potassium contents). This model has a thermal boundary between the upper and lower mantles and a hot mantle which, nevertheless, is far below the inferred melting point (light solid and dashed curves). Model B has the same amount of radioactivity, but it is distributed between two chemically distinct upper mantle reservoirs. This model approaches the melting point at the top of the depleted layer (layer 2) and has lower temperatures and higher viscosities in the lower mantle. A perturbation of geotherm B by, for example, continental insulation or a convectively induced uplift of the chemical boundary, will cause melting in layer 2. Geotherm A is modified from (*40*).

16.14

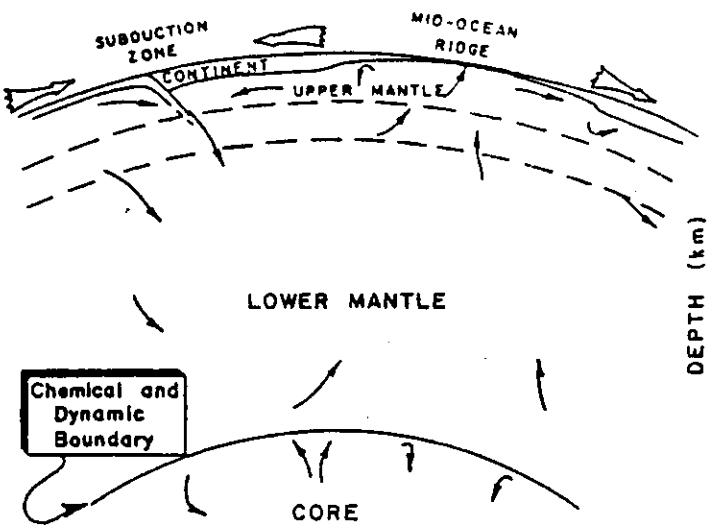

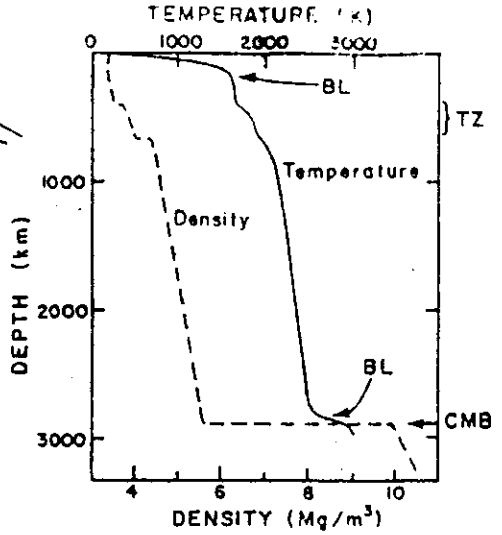

16.15

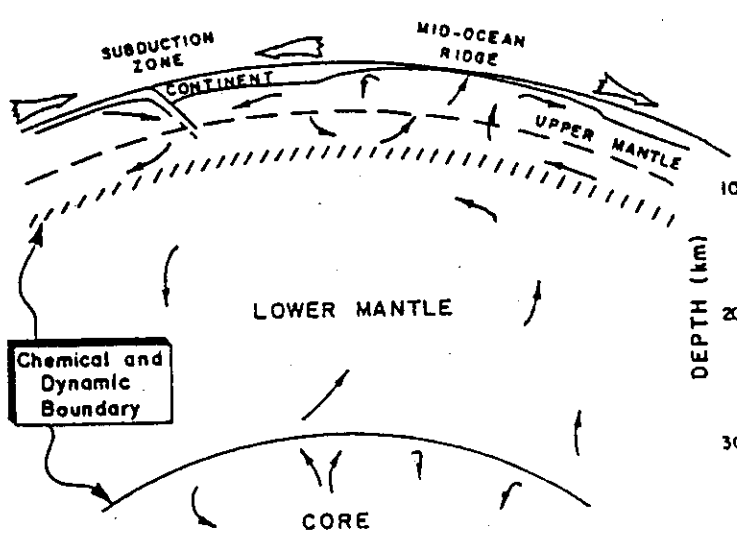

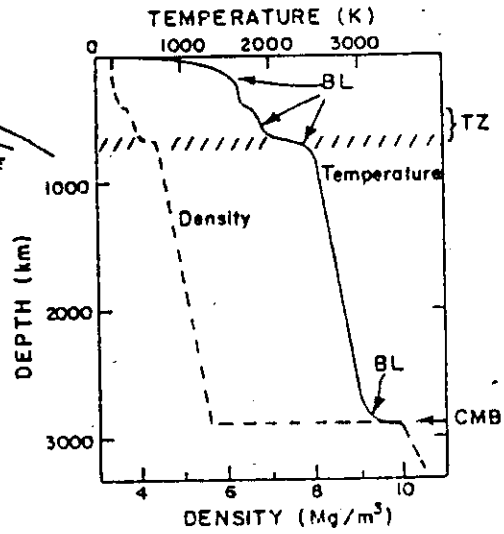

Jeanloz 1981a
Proc. Am. Chem Soc. 70

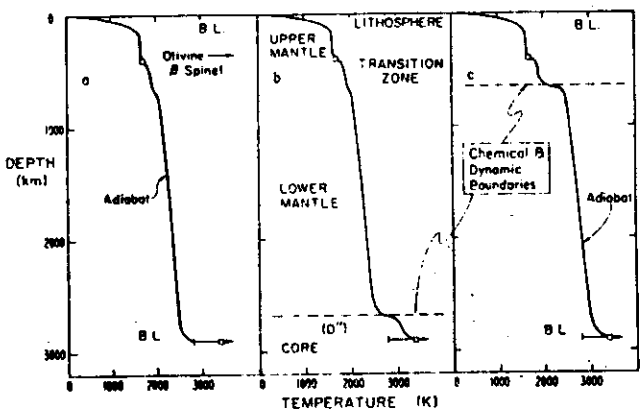

16.16

Fig. 6. Temperature profiles through the earth's mantle: three acceptable models. Thermal boundary layers (BL) are indicated in the upper and lower mantle, while dynamic barriers associated with possible chemical transitions in the lower mantle are shown as dashed lines. The preferred core temperature and its plausible lower bound are also shown. Note the fundamental asymmetry of the profiles caused by the large decrease in temperature through the lithosphere, an effect which has no counterpart at depth within the earth and which is due to temperature-dependent rheology. (*a*) Adiabat through lower mantle with one thermal boundary layer at the core-mantle boundary and with the core at a relatively low temperature. Taken from Figure 2. (*b*) Adiabat with two thermal boundary layers near the base of the mantle corresponding to a seismologically complex and chemically distinct *D"* region. (*c*) Adiabat with a thermal boundary layer at the top and the bottom of the lower mantle. In this case the lower and upper mantle are separate chemical and dynamic systems.

Jeanloz Richter 1979
J.G.R. 84 5497-5504

16.15

16.16

REFERENCES

Ahrens, T.J., and Schubert, G. (1975) Gabbro-eclogite reaction rate and its geophysical significance. Revs. Geophys. Space Phys. 13, 383-400.

Akaogi, M., and Akimoto, S. (1977) Pyroxene-garnet solid-solution equilibria in the systems $Mg_4Si_4O_{12}$-$Mg_3Al_2Si_3O_{12}$ and $Fe_4Si_4O_{12}$-$Fe_3Al_2Si_3O_{12}$ at high pressures and temperatures. Phys. Earth Planet. Inter. 15, 90-106.

Akimoto, S., and Fujisawa, H. (1968) Olivine-spinel solid solution equilibria in the system Mg_2SiO_4-Fe_2SiO_4. J. Geophys. Res. 73, 1467-1479.

Akimoto, S., Akaogi, M., Kawada, K., and Nishizawa, O. (1979) Mineralogic distribution of iron in the upper half of the transition zone in the earth's mantle, in ^The Geophysics of the Pacific Ocean Basin and Its Margin^, Geophys. Monogr. Ser., vol 19, edited by G.H. Sutton, M. H. Manghnani, and R. Moberly, pp. 399-405, AGU, Washington, D.C.

Akimoto, S., Matsui, Y., and Syono, Y, (1976) High pressure crystal chemistry of orthosilicates and formation of the mantle transition zone. pp. 327-263. ^in^ ^The physics and chemistry of minerals and rocks^ ed. R.G. J. Strens, John Wiley, London.

Anderson, D.L. (1984) The Earth as a planet: Paradigms and paradoxes. Science, 223, 347-355.

Anderson, D.L. (1976) The 650 km mantle discontinuity. Geophys. Res. Lett. 3, 347-349.

Anderson, D.L. (1979) The upper mantle: Eclogite? Geophys. Res. Lett. 6, 433-436.

Bass, J.D., and Anderson, D.L. (1984) Mantle composition and mineral elasticity (in press)

Bernal, J.D. (1936) Discussion. Observatory, 59, 268.

Binns, R.A., Davis, R.J., and Reed, S.B.J. (1969) Ringwoodite, natural $(Mg,Fe)_2SiO_4$ spinel in the Tenham meteorite. Nature, London, 221,943-944.

Birch, F. (1964) Density and composition of mantle and core. J. Geophys. Res. 69, 4377-4388.

Brown, J.M., and McQueen, R.G., (1982) The equation of state for iron and the Earth's core. pp. 611-623, ^in^ ^High pressure research in geophysics^, ed. S. Akimoto and M.H. Manghnani, Reidel Publ. Co Amsterdam.

Brown, J.M., Ahrens, T. J., and Shampine, D.L. (1984) J. Geophys. Res. (in press)

Bullen, K.E. (1936) The variation of density and the ellipticities of strata of equal density within the earth. Mon. Nor. R. astron. Soc., Geophys. suppl., 3, 395-401.

Clark, S.P. and Ringwood, A.E. (1964) Density distribution and constitution of the mantle. Rev. Geophys. 2, 35-88.

Davies, G.F. (1980) Thermal histories of convective earth models and constraints on radiogenic heat production in the earth. J. Geophys. Res. 85, 2517-2530.

Davies, G.F., and Gaffney, E. (1973) Identification of high pressure phases of minerals and rocks from Hugoniot data. Geophys. J. 33, 165-183.

DePaolo, D.J. (1980) Crustal growth and mantle evolution: Inference from models of element transport and Nd and Sr isotopes. Geochim. Cosmochimica. Acta. 44,1185-1196.

DePaolo, D.J., and Wasserburg, G.J. (1976) Inferences about magma sources and mantle structure from variations of $^{143}Nd/^{144}Nd$. Geophys. Res. Lett. 3, 743-746.

Drickamer, H.G., and Frank, C.W. (1973) ^Electronic transitions and the high pressure chemistry and physics of solids^. Chapman and Hall, London.

Fujisawa, H. (1968) Temperature and discontinuties in the transition layer within the earth's mantle: Geophysical application of the olivine-spinel transition in the Mg_2SiO_4-Fe_2SiO_4 system. J. Geophys. Res. 73, 3281-3294.

Fukao, Y. (1977) Upper mantle P-structure and the 650 km discontinuity, pp151-161 ^in^ ^High Pressure Research^, ed. M.H. Manghnani, and S. Akimoto, Academic Press, New York, 1977.

Fukao, Y., Nagahashi, T., and Mori, S. (1982) Shear velocity i the mantle transition zone, pp 285-300, ^in^ S. Akimoto and M.H. Nagnhuani (eds). ^High Pressure Research in Geophysics^ Center for Academic Pubs. Tokyo, Japan (632 pp) Reidel Pub.Co. Amsterdam

Goldschmidt, V.M. (1931) Zur Kristallochemie des Germaniums. Nach. Akad. wiss. Goettingen, math. phys. kl. 1, 184-190.

Hamaya, N., and Akimoto, S. (1982) Experimental ivestigation on the mechansim of olivine-spinel transformation: Growth of single crystal spinel from single crystal olivine i Ni_2SiO_4. pp 373-390, ^in^ S. Akimoto and M.H. Nagnhuani (eds). ^High Pressure Research in Geophysics^ Center for Academic Pubs. Tokyo, Japan (632 pp) Reidel Pub.Co. Amsterdam

Harris, P.G., Reay, A., and White,, I.G. (1967) Chemical compostion of the upper mantle. J. Geophys. Res. 72, 6359-6369.

Hazen, R.M., and Finger, L.W. (1982) ^Comparative Crystal Chemistry^, John Wiley and Son, New York, 231 pp.

Horiuchi, H., Akaogi, M., and Sawamoto, H. (1982) Crystal structure . studies on spinel-realted phases, spinelloids:Implications to olivine-spinel phase transformation and systematics, pp. 391-403, ^in^ S. Akimoto and M.H. Nagnhuani (eds). ^High Pressure Research in Geophysics^ Center for Academic Pubs. Tokyo, Japan (632 pp) Reidel Pub.Co. Amsterdam

Hornstra, J. (1961) Dislocations, stacking faults ad twins in the spinel structure ^in^ ^Proc. IVth Inst. Symp. of the Reactivity od Solids^, ed J.H. DeBoer, pp.563-570, Elsevier, Amsterdam.

Houseman, G.A., McKenzie, D.P. and Molnar, P. (1981) Convective instability of a thickened boundary layer and its relevance for thermal evolution of continental convergent belts. J. Geophys. Res. 86, 6115-6132.

Ito, E., and Yamada, H. (1982) Stability realtions of silicate spinels, ilmenites, and perovskites, ^in^ ^High pressure research in Geophysics^ eds. S. Akimoto, and M.H. Manghnani, pp.405-419. Center for Academic Publishing, Tokyo.

Ito, E., Takahashi, E., and Matsui, Y. (1984) The mineralogy and chemistry of the lower mantl; An implication of the ultrahigh-pressure phase relations in the system MgO-FeO-SiO_2. Earth Planet. Sci. Lett. 67, 238-248.

Ito, K., and Kennedy, G.C. (1970) The fine structure of the Basalt-eclogite transition. Min. Soc. Amer. Spec. Pap. 3, 77-83.

Jayaraman, A. (1984) The diamond anvil high pressure cell. Sci. American. 250, 42-50.

Jeanloz, R. (1982) Oxygen in the Earth's metallic core?. Nature, 299, 108-109.

Jeanloz, R. (1983) The Earth's core. Sci. American. 249, 56-65. High pressure chemistry of the Earth's mantle and core ^in^ ^Mantle Convection^, ed. W.R. Peltier (in press).

Jeanloz, R (1984) High pressure chemistry of the Earth's mantle and core ^in^ ^Mantle Convection^, ed. W.R. Peltier (in press). Jeanloz, R., and Richter, F. M. (1979) Convection, composition, and the thermal state of the lower mantle. J. Geophys. Res. 84, 5497-5504.

Jeanloz, R., and Thompson, A.B. (1983) Phase transitions and mantle discontinuities. Revs. Geophys. Space Phys. 21, 51-74.

Jordan, T.H. (1977) Lithosphere slab penetration into the lower mantle beneath the Sea of Okhotsk. Geophys. J. 3, 473-496.

Kamb, B. (1968) Structural basis of the olivine-spinel stability relation. Amer. Mineral. 53, 1439-1455.

Kennedy, G.C. (1959) The origin of continents, mountain ranges and ocean basins. Amer. Sci. 147, 491-504.

Verhoogen, J. (1980) ^Energetics of the Earth^ Nat. Acad. Sciences, Washington, D.C., 139 pp.

Kushiro, I., Syono, Y., and Akimoto, S. (1967) Stability of phlogopite at high pressures and possible presence of phlogopite in the Earth's upper mantle. Earth Planet. Sci. Lett. 3, 197-203.

Langan, R.T., and Sleep, N.H. (1982) A kinematic thermal history of the Earth's mantle. J. Geophys. Res. 87, 9225-9235.

Lees, A.C., Bukowski, M.T., and Jeanloz, R. (1983) Reflection properties of phase transition and compostional change models of the 670 km discontinuity. J. Geophys. Res. 88, 8145-8159.

Liu, L. (1976) The high pressure phases of $MgSiO_3$. Earth Planet. Sci. Lett. 31, 200-208.

Liu. L. (1979) Phasé transformations and constitution of the deep mantle in The Earth: Its Orogin, Structure and Evolution, edited by M.W. McElhinny, pp. 177-202, Academic Press, New York.

Liu, L.G. (1982) High-pressure phase transformations of the dioxides: Implications for structure of SiO_2 at high pressure. pp 349-360, ^in^ S. Akimoto and M.H. Magnhuani (eds). ^High Pressure Research in Geophysics^ Center for Academic Pubs. Tokyo, Japan (632 pp) Reidel Pub.Co. Amsterdam

Lovering, J.F. (1958) The nature of the Mohorovicic discontinuity EOS, Trans. Amer. Geophys. Union, 39, 947-955.

Mao, H. K. and Bell, P.M. (1977) Disproportionation equilibrium in iron-bearing systems at pressures above 100 kbar with applications to chemistry of the earth's mantle. p. 236-249 ^in^ ^Energetics of geological processes^, eds. S.K. Saxena, and S. Bhattacharji, Springer, New York, 473 pp.

McQueen, R.G., Marsh, S.P., and J.N. Fritz (1967) Hugoniot equation of state of twelve rocks. J. Geophys. Res. 72, 4999-5036.

Ming, L.C., and Bassett, W.A. (1975) Decomposition of $FeSiO_3$ into $FeO + SiO_2$ under very high pressure and high temperature. Earth Planet. Sci. Lett. 25, 68-70.

Ming, L.C., and Manghuani, M.H. (1982) High-pressure transformations in rutile-structural dioxides, pp., 329-347, ^in^ S. Akimoto and M.H. Magnhuani (eds). ^High Pressure Research in Geophysics^ Center for Academic Pubs. Tokyo, Japan (632 pp) Reidel Pub.Co. Amsterdam

O'Hara, M.J. (1970) Upper mantle composition inferred from laboratory experiments and observation of volcanic products. Phys. Earth Planet. Inter. 3, 236-245.

O'Nions, R.K., Carter, S.R., Evensen, N.M., and Hamilton, P.J. (1979) Geochemical and cosmochemical application of Nd-isotopes. Ann. Revs. Earth Planet. Sci. 7, 1-31.

Poirier, J.P. (1981) On the kinetics of the olivine-spinel transition. Phys. Earth Planet. Inter. 26, 179-187.

Press, F. (1969) The suboceanic mantle. Science, 165, 174-176.

Reid, A.F., and Ringwood, A.E. (1970) The crystal chemistry of dense M_3O_4 polymorphs: High pressure Ca_2GeO_4 of K_2NiF_4 structure type. J. Solid State Chem. 1, 557-565.

Richardson, S.W., and England, P.C. (1979) Metamorphic consequences of crustal-eclogite production in overthrust orogenic zones. Earth Planet. Sci. Letts. 42, 183-190.

Richards, P.G. (1972) Seismic waves reflected from velocity gradient anomalies within the earth's upper mantle. Z. Geophys. 38, 517-527.

Richter, F.M., and Ribe, N.M. (1979) On the importance of advection in determining the local isotopic compostion of the mantle. Earth Planet. Sci. Lett. 43, 212-222.

Richter, F.M., and McKenzie, D.P. (1981) On some consequences and possible causes of layered mantle convection. J. Geophys. Res. 86, 6133-6142.

Ringwood, A.E., (1970) Phase transformations and the constitution of the mantle. Phys. Earth. Planet. Inter. 3, 109-155.

Ringwood, A.E. (1975) Composition and Petrology of the Earth's Mantle, 618 pp., McGraw-Hill, New York.

Ringwood, A.E. (1978) ^Origin of the Earth and Moon^, Springer Verlag, New York.

Ringwood, A.E. (1982) Phase transformations and differentiation in suducted lithosphere: Implication for mantle dynamics, basalt petrogenesis, and crustal evolution. J. Geol. 90, 611-643.

Ringwood, A.E., and Green D.H. (1966) An experimental investigationof the gabbro-eclogite transformation and some geophysical implications. Tectonophys. 3, 383-427.

Ringwood, A.E., Major, A. (1966a) Synthesis of Mg_2SiO_4- Fe_2SiO_4 solid solutions. Earth Planet Sci. Letts. 1, 241-245.

Ringwood, A. E., and Major, A. (1966b) High pressure transformation of $FeSiO_3$ pyroxene to spinel plus stishovite. Earth Planet. Sci. Letts. 1, 135-136.

Ringwood, A.E., and Major, A. (1970) The system Mg_2SiO_4- Fe_2SiO_4 at high pressures and temperatures. Phys. Earth Planet. Inter. 3, 109-115.

Rubie, D.C. (1984) The olivine-spinel transformation and the rheology of subducting lithosphere. Nature, 308, 305-508.

Schubert, G., Stevenson, D., and Cassen, P. (1980) Whole planet cooling and the radiogenic heat source contents of the earth and moon. J. Geophys. Res. 85, 2531-2538.

Spohn, T., and Schubert, G. (1982) Modes of mantle convection and the removal of heat from the Earth's interior. J. Geophys. Res. 87, 4682-4696.

Stewart, R.M. (1973) Composition and temperature of the outer core. J. Geophys. Res. 78, 2586-2597.

Stevenson, D.J. (1981) Models of the Earth's Core, Science 214, 611-619.

Sung, C.M., and Burns, R.G. (1976) Kinetics of high-pressure phase transformation: Implications to the evolution of the olivine-spinel transition in the downgoing lithosphere and its consequences ion the dynamics of the mantle. Tectonophys. 31, 1-32.

Sung, C.M., and Burns, R.G. (1978) Crystal structural features of the olivine-spinel transition. Phys. Chem. Minerals. 2, 177-197.

Whitcomb, J., and Anderson, D.L. (1970) Reflection of p'p' seismic waves from discontiuties i the matle. J. Geophys. Res. 75, 5713-5728.

Yagi, T., Bell, P.M., and Mao, H.-K. (1979) Phase relations in the system MgO-FeO-SiO_2 between 150 and 700 kbar at 1000°C. Carnegie Inst. Washington Year Book. 78, 614-618.